Published in final edited form as:

FEBS J. 2018 January ; 285(1): 72–86. doi:10.1111/febs.14313.

Fyn-dependent phosphorylation of PlexinA1 and PlexinA2 at conserved tyrosines is essential for zebrafish eye development

Riley M. St. Clair, **Sarah E. Emerson**, **Kristen P. D'Elia**, **Marion E. Weir**, **Anna M. Schmoker**, **Alicia M. Ebert***, and **Bryan A. Ballif***

Department of Biology, University of Vermont, Burlington, VT 05405, USA

Abstract

Plexins (Plxns) are semaphorin (Sema) receptors that play important signaling roles, particularly in the developing nervous system and vasculature. Sema-Plxn signaling regulates cellular processes such as cytoskeletal dynamics, proliferation, and differentiation. However, the receptor-proximal signaling mechanisms driving Sema-Plxn signal transduction are only partially understood. Plxn tyrosine phosphorylation is thought to play an important role in these signaling events as receptor and non-receptor tyrosine kinases have been shown to interact with Plxn receptors. The Src-family kinase Fyn can induce the tyrosine phosphorylation of PlxnA1 and PlxnA2. However, the Fyn-dependent phosphorylation sites on these receptors have not been identified. Here, using mass spectrometry-based approaches, we have identified highly-conserved, Fyn-induced PlxnA tyrosine phosphorylation sites. Mutation of these sites to phenylalanine results in significantly decreased Fyn-dependent PlxnA tyrosine phosphorylation. Furthermore, in contrast to wildtype human *PLXNA2* mRNA, mRNA harboring these point mutations cannot rescue eye developmental defects when co-injected with a *plxnA2* morpholino in zebrafish embryos. Together these data suggest that Fyn-dependent phosphorylation at two critical tyrosines is a key feature of vertebrate PlxnA1 and PlxnA2 signal transduction.

Graphical Abstract

*Corresponding Authors. Alicia M. Ebert, Ph.D., Bryan A. Ballif, Ph.D., Address: Department of Biology, University of Vermont, 109 Carrigan Drive, 120A Marsh Life Sciences, Burlington, VT 05405, USA, Fax: +1.802.656.2914, Telephone (A.M.E.): +1.802.656.0458, Telephone (B.A.B.): +1.802.656.1389, amebert@uvm.edu, bballif@uvm.edu.

Author Contributions

RMS planned experiments, performed experiments, analyzed data and wrote the manuscript. SEE, KPD, MEW and AMS performed experiments and analyzed data. AME planned experiments and analyzed data. BAB planned experiments, analyzed data and wrote the manuscript.

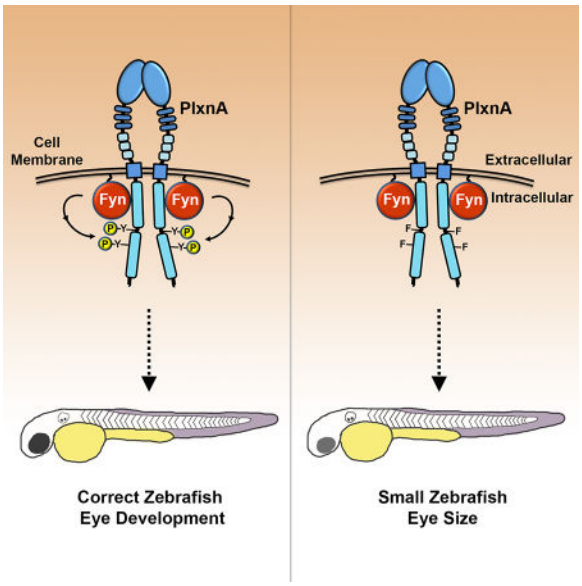

PlxnA receptors regulate many processes including proper nervous system development. However, their receptor-proximal signaling mechanisms are only partially understood. Using mass spectrometry and biochemistry, we identify two Fyn-induced PlxnA tyrosine (Y) phosphorylation sites. These phosphorylation sites are necessary for signaling *in vivo* as wildtype but not tyrosine-to-phenylalanine (F) mutant PLXNA2 mRNA can rescue the small-eye phenotype of *plxnA2* morphant zebrafish.

Keywords

Fyn; Mass Spectrometry; Phosphorylation; Plexin; Semaphorin

1. Introduction

Plexins (Plxns) are semaphorin (Sema) receptors that are highly expressed during development where Sema-Plxn signaling plays important roles in nervous system, cardiac, vasculature and bone development [1, 2]. At the cellular level, Sema-Plxn signaling regulates cytoskeletal dynamics, integrin-mediated adhesion, proliferation, differentiation, transcription, and programmed cell death [3–7]. With a wide array of functions, the signaling outcome of Semas depends on a variety of factors, including receptor subtype and the effector proteins associated with the cytosolic regions of both Plxns and transmembrane Semas [2, 8]. The intracellular signaling milieu in which Plxns and Semas act is highly dynamic and determined by differential protein expression driven by changing cell types and developmental timing [9–11].

In mammals, there are nine Plxns classified into four subfamilies: PlxnA1–A4, B1–3, C1, and D1 [12]. PlxnA family members, receptors for Sema3, Sema5, and Sema6 classes, are the most highly expressed Plxns throughout nervous system development, with PlxnA2 being the most highly expressed PlxnA in the cortical plate [12–17]. Furthermore, PlxnA2 and the close family member PlxnA1 are also expressed in non-cortical regions of the

nervous system, including the retina [14, 18]. We have previously shown the importance for Sema6-PlxnA signaling in early vertebrate eye development, as decreasing PlxnA2 or Sema6A in the zebrafish results in reduced retinal precursor cell proliferation, loss of eye field cohesion, and impaired retinal lamination [7, 18]. Together, these results show that Sema6-PlxnA signaling initiates a variety of functional outcomes depending on cellular and organismal context.

Although the nature of Sema-Plxn binding has been well characterized [19, 20], the receptor proximal events that initiate specific functional outcomes of Sema-Plxn signaling are only partially understood. Plxn phosphorylation by tyrosine kinases is thought to be one way by which Plxns mediate intracellular signaling in response to Sema binding [21]. Receptor-type and cytoplasmic tyrosine kinases are known to associate with Plxn family members [16, 22–24]. In fact, there is evidence through large-scale proteomic screens that the intracellular domain of all nine Plxn family members can be tyrosine phosphorylated at least to some degree [25]. However, currently only PlxnB, based on mutagenesis studies, has been shown to be phosphorylated at specific sites by a specific kinase (ErbB2) [26] and to our knowledge no kinases have been identified to phosphorylate specific PlxnA tyrosine residues. Nonetheless, PlxnA receptors have been shown to be tyrosine phosphorylated when overexpressed in standard human cell lines [12] and the Src family tyrosine kinase (SFK) Fyn was later discovered to constitutively associate with and phosphorylate the intracellular region of PlxnA1 and PlxnA2 [22]. Furthermore, the cytosolic tyrosine kinase Fes has been shown to bind and phosphorylate PlxnA1 [23], and the receptor tyrosine kinase (RTK) VEGFR2 has been shown to associate with PlxnA1 [16, 24].

In spite of these known associations between tyrosine kinases and PlxnA receptors, no tyrosine phosphorylation sites have been identified to be regulated by specific tyrosine kinases. As Fyn has been implicated in PlxnA phosphorylation and is critical to Sema-induced dendritic maturation in cultured cortical neurons [22, 27], we focused our study on Fyn-dependent PLXNA phosphorylation. To begin to elucidate the signaling role of tyrosine phosphorylation sites on Plxns, we set out to ascertain Fyn-dependent phosphorylation sites of PLXNA2 and PLXNA1. Using mass spectrometry and biochemical approaches, we have identified two novel Fyn-induced PLXNA phosphorylation sites that are conserved across vertebrates and invertebrates. Site-specific mutants of PLXNA2 and PLXNA1 verified that these tyrosine residues are the major sites of Fyn-dependent phosphorylation. Using zebrafish as a model organism, we investigated the *in vivo* functional significance of these sites and found that Fyn-dependent PlxnA2 phosphorylation is critical for zebrafish eye size. We end with a discussion on the possible signaling roles of these phosphorylation events at the molecular and cellular levels.

2. Results

2.1. Fyn Induces PLXNA2 and PLXNA1 Tyrosine Phosphorylation

To recapitulate the Fyn-dependent PlxnA2 and PlxnA1 phosphorylation found by Sasaki *et al.* 2002, we first transfected HEK293 cells with expression plasmids encoding Flag-tagged PLXNA2 and either Fyn wildtype (WT) or a kinase dead (KD) point mutant of Fyn. PLXNA2 showed prominent tyrosine phosphorylation when Fyn WT was co-expressed and

this phosphorylation was absent when Fyn KD was co-expressed (Fig. 1A). Similarly, Flag-tagged PLXNA1 tyrosine phosphorylation was present when Fyn WT was co-expressed and absent when Fyn KD was co-expressed (Fig. 1B). These results are consistent with the findings of others (Sasaki et al., 2002) and demonstrate tyrosine phosphorylation events on PlxnA2 and PlxnA1 that are induced by Fyn kinase activity. To understand the molecular mechanisms of how PlxnA tyrosine phosphorylation might regulate PlxnA receptors, we next sought out to identify the tyrosine residues on PLXNA2 and PLXNA1 that are phosphorylated in a Fyn-dependent manner.

2.2. Bioinformatics Reveals Conserved Tyrosine Phosphorylation Sites on PLXNA2 and PLXNA1

As an initial approach to identify potential Fyn-dependent tyrosine phosphorylation sites we asked if PlxnA family members were known to be tyrosine phosphorylated at specific sites as determined by large-scale phosphoproteomic analyses. PhosphoSitePlus [25] is an online database that curates post-translational modification information, including phosphorylation, from both large-scale and site-specific studies. PhosphoSitePlus listed eight intracellular tyrosine residues found to be phosphorylated on PLXNA2 in large-scale proteomic screens. Seven out of these eight residues were found phosphorylated two or fewer times. However, Y1605 has been found phosphorylated in 20 independent proteomic screens (Fig. 2A). This site is conserved across vertebrates and invertebrates as well as within PLXNA1 (Fig. 2B). Indeed, PhosphoSitePlus shows nine intracellular tyrosine residues to be phosphorylated on PLXNA1, with eight of these sites only being found to be phosphorylated once (Fig. 2A). However, Y1608 in PLXNA1 is homologous to PLXNA2 Y1605 and has been found to be phosphorylated 58 independent times. These data suggest there may be an evolutionarily conserved role for this phosphorylation event in PlxnA signaling. Importantly, the kinase that phosphorylates this site has not been identified and we hypothesized that Fyn could be the tyrosine kinase responsible for phosphorylating PlxnA2 and PlxnA1 on Y1605 and Y1608, respectively.

2.3. Targeted Mass Spectrometry Finds Y1605 as a Fyn-Dependent Phosphorylation Site on PLXNA2

To determine if Fyn phosphorylates PLXNA2 at Y1605 we made use of synthetic, stable isotope-containing peptides harboring phosphorylated and unphosphorylated Y1605 as references to determine the expected elution time of the native PLXNA2 peptides as well as their MS2 spectral patterns. HEK293 cells were transfected with expression plasmids encoding PLXNA2 WT-Flag alone or with either Fyn WT or Fyn KD. PLXNA2 was then immunopurified from extracts of each group. A portion of each immunoprecipitation was used for immunoblotting to confirm PLXNA2 expression and to confirm Fyn-induced PLXNA2 tyrosine phosphorylation (Fig. 3A). The majority of each immunoprecipitation was subjected to SDS-PAGE and coomassie staining (Fig. 3B). From these gels, the control and PLXNA2 bands running at approximately 200 kDa were excised and subjected to in-gel tryptic digestion. Extracted peptides were supplemented with unphosphorylated and phosphorylated Y1605-containing peptides (QTSSYNIPASASISR) containing $^{13}C_5$- and ^{15}N-labeled proline. A targeted approach was used to trigger MS/MS scans on the *m/z* values of the doubly-charged precursor ions for the native tryptic peptides of PLXNA2

containing unphosphorylated and phosphorylated Y1605. Using the synthetic stable isotope-containing peptides as a reference allowed us to readily detect the phosphorylated and unphosphorylated Y1605-containing PLXNA2 tryptic peptides (the MS2 spectral pattern of the phosphorylated synthetic peptide is shown in Fig. 3C). The unphosphorylated peptide was found across treatment groups. However, the phosphorylated Y1605 PLXNA2 peptide was only detected in cells expressing both PLXNA2 and Fyn WT (Fig. 3D). This supports the hypothesis that active Fyn can induce phosphorylation of PLXNA2 at Y1605 in cells.

2.4. A SILAC Mass Spectrometry Approach Identifies Y1677 as a Novel Fyn-Dependent Phosphorylation Site on PLXNA2

To ascertain if additional Fyn-dependent PLXNA2 phosphorylation sites could be identified, we used Stable Isotope Labeling of Amino Acids in Cell Culture (SILAC), a proteomics approach that utilizes cells grown in media containing heavy-labeled amino acids [28]. The advantage of a quantitative labeling method such as SILAC is that it allows different treatment types to be combined and handled equally in the preparation of peptides for LC-MS/MS. HEK293 cells expressing PLXNA2 WT-Flag and Fyn WT were grown in DMEM containing no heavy labeled amino acids (Light condition, Fig. 4A). Cells expressing PLXNA2 WT-Flag and Fyn KD were grown in DMEM containing ^{13}C- and ^{15}N- labeled arginine and lysine (Heavy condition), resulting in newly synthesized proteins incorporating heavy labels. PLXNA2 was immunoprecipitated using α-Flag resin and both PLXNA2 groups were combined and loaded onto a SDS-PAGE gel and stained with coomassie dye (Fig. 4B). The PLXNA2 band as well as the untransfected control band were cut and prepared for mass spectrometry analysis.

Following a SEQUEST search and an automated calculation of the heavy:light ratio [29] of PLXNA2 peptides, we determined the distribution of all PLXNA2 fully tryptic peptides identified which covered amino acid sequences for which we did not find a phosphorylation event. As the relative abundance of these peptides was not likely altered by the treatment, they would define the relative amount of PLXNA2 immunoprecipitated from the two conditions. The average heavy:light ratio for the 71 peptide pairs we identified was 2.9 with a standard deviation of 0.5. This indicated that in this experiment the amount of PLXNA2 immunoprecipitated from the heavy state with Fyn KD expressed was nearly three times the amount immunoprecipitated from the light state with Fyn WT expressed. Only one phosphotyrosine-containing peptide was identified in our analysis and, importantly, it was found only in the light state. Surprisingly, we did not identify phosphotyrosyl-1605 in the SILAC analysis. The identified phosphopeptide contained tyrosine phosphorylation at Y1677. The stoichiometry of phosphorylation at Y1677 can be inferred by the decrease in the unphosphorylated form of this peptide relative to the average SILAC ratio. The SILAC ratio of the unphosphorylated form is approximately 15% less when Fyn WT is co-expressed compared to the mean SILAC ratio of PLXNA2 peptides suggesting 15% phosphorylation at that site (Fig. 4C). As the precursor ion for the phosphopeptide was not observable in the heavy state, a signal-to-noise (S/N) calculation was used to approximate its minimum fold increase. While the total amount of the phosphopeptide might in fact be zero, the S/N calculation describes the lowest possible observable signal and serves as a baseline for the minimum fold increase. The lowest possible signal is a peptide ion in the full MS1 mass

spectrum with an observable isotopic envelope as compared to surrounding noise peaks which do not have observable isotopic envelopes and therefore are considered noise from the solvent alone. In this case the signal of the observed light phosphopeptide was 9.4 times the noise. Given that less light PLXNA2 was immunoprecipitated compared to heavy PLXNA2, the total fold increase of this phosphopeptide induced by Fyn WT was even greater.

Interestingly, a multiple species alignment indicates that Y1677 is conserved between PlxnA2 and PlxnA1 across species, including vertebrates and invertebrates (Fig. 3E). Indeed, this tyrosine residue is in a highly conserved region of the cytoplasmic domain across all Plxn family members [21], which may point to an evolutionarily important function.

2.5. Y1605 and Y1677 are the Major Fyn-dependent Sites of PLXNA2 Tyrosine Phosphorylation

To determine if Y1605 and Y1677 were the major sites of Fyn-dependent PLXNA2 tyrosine phosphorylation we made single and double tyrosine-to-phenylalanine substitutions in PLXNA2 at these sites (Y1605F, Y1677F, and Y1605F/Y1677F (Y2F)). Co-transfection of expression plasmids encoding PLXNA2 Y2F-Flag and Fyn WT showed a significant decrease in Fyn-dependent PLXNA2 tyrosine phosphorylation (Fig. 5A, quantified in Fig. 5C). However, some Fyn-dependent tyrosine phosphorylation remained on the Y2F mutant suggesting the presence of at least one additional Fyn-dependent tyrosine phosphorylation site on PLXNA2. To determine the predominant Fyn-induced PLXNA2 phosphorylation site, the single point mutants were co-expressed in HEK293 cells with Fyn WT. We found that Fyn-induced tyrosine phosphorylation was reduced for both Y1605F and Y1677F mutants (Fig. 5B, quantified in Fig. 5C). Interestingly, each PLXNA2 mutant appeared to decrease in tyrosine phosphorylation signal equally, suggesting Fyn shows roughly equal preference for phosphorylating Y1605 and Y1677.

2.6. Fyn-Dependent Phosphorylation Sites are Conserved between PLXNA1 and PLXNA2

To ascertain if Fyn phosphorylates PLXNA1 at sites homologous to those identified on PLXNA2, we co-transfected HEK293 cells with expression plasmids encoding Fyn WT and either PLXNA1 WT-Flag or PLXNA1 Y2F-Flag. The Y2F allele of PLXNA1 has tyrosine-to-phenylalanine substitutions at Y1608 and Y1679, the sites homologous to Y1605 and Y1677 in PLXNA2. As hypothesized, PLXNA1 tyrosine phosphorylation decreased significantly when both Y1608 and Y1679 were unable to be phosphorylated (Fig. 6A, quantified in Fig. 6B). In fact, it appears that the combination of Y1608 and Y1679 constitute almost all of the Fyn-dependent tyrosine phosphorylation on PLXNA1 (Fig. 6A).

2.7. Fyn-dependent PlxnA2 Phosphorylation Sites are Critical for Zebrafish Eye Development

To investigate the functional importance of *in vivo* PlxnA2 phosphorylation, we turned to the zebrafish model as we have previously characterized the function of PlxnA2 in zebrafish eye development [7, 18]. *PlxnA2* is expressed in the retina and is critical to zebrafish eye development, as decreasing endogenous PlxnA2 using a morpholino anti-sense oligonucleotide (MO) targeted to *plxnA2* results in decreased proliferation of retinal

precursor cells (RPCs), loss of RPC cohesion within migrating optic vesicles, impaired retinal lamination, and decreased eye size [7, 18]. Importantly, these phenotypes are rescued by co-injecting the *plxnA2* MO with human *PLXNA2-WT* mRNA at the one-cell stage of development, supporting the evolutionary conservation of PlxnA2 among vertebrates [7, 18]. The *plxnA2* MO construct used has been previously validated to address knock-down specificity and any potential off-target effect [7, 18]. If PlxnA phosphorylation is critical to Sema6A signaling and vertebrate eye development, we hypothesized that the *plxnA2* morphant phenotypes would not be rescued upon co-injection of *plxnA2* MO with human *PLXNA2 Y2F* mRNA. Indeed, while co-injecting *plxnA2* MO with *PLXNA2 WT* mRNA rescued the small eye phenotype at 48 hours post fertilization (hpf), co-injection of *PLXNA2 Y2F* mRNA did not (Fig. 7A–D). To control for any variations in overall embryo size we normalized eye diameter to head length (quantified in Fig. 7G). Furthermore, overexpression of human *PLXNA2 WT* or *Y2F* mRNA resulted in no obvious phenotype, nor was eye size significantly different than uninjected controls (UIC) (Fig. 7E–F; quantified in 7G). As it was formally possible that PLXNA2 Y2F did not rescue the *plxnA2* MO phenotype due to improper subcellular localization, we conducted immunofluorescence on HEK293, COS7, and NIE-115 cells expressing PLXNA2 WT and Y2F (Fig. 7H–O). HEK293 and COS7 cells were relevant given they have been used to investigate PlxnA2 signaling in biochemical and cell-based assays [12, 15, 19, 20]. COS7 cells are heterogeneous and we focused here on cells with extended processes as Sema-PlxnA signaling is known to localize to neuronal processes and to regulate axon and dendrite guidance [12, 30–32]. NIE-115 is a heterogeneous cell line that is responsive to semaphorins, as Sema3A stimulation results in neurite retraction [33]. We show immunofluorescence of PLXNA2 WT and Y2F expressed in NIE-115 cells displaying long processes (Fig. 7L,M) as well as numerous short processes (Fig. 7N,O). In all cases PLXNA2 WT and Y2F appeared to have similar subcellular expression patterns (Fig. 7H–O), suggesting that the Y2F mutation did not affect protein localization. Together, these results suggest that the Fyn-dependent PlxnA phosphorylation sites identified in this study have important, conserved *in vivo* functions.

3. Discussion

Here we show that Fyn induces the phosphorylation of two conserved sites on PLXNA1 and PLXNA2. Mechanistically, PlxnA tyrosine phosphorylation by SFKs could, via structural alterations, modulate the GAP activity of the receptors as the conserved sites of tyrosine phosphorylation are in or near the split GAP domain of the PlxnA receptors [34]. Additionally, PlxnA tyrosine phosphorylation could be involved in recruiting effectors of signal transduction. Tyrosine phosphorylation can regulate protein-protein interactions by providing docking sites for SH2 or PTB domain-containing proteins. Precedence for these signaling mechanisms have been established in Sema-Plxn signaling with Sema4D-induced tyrosine phosphorylation of PlxnB1 leading to the recruitment of the p85 subunit of PI3K and subsequent Akt activation. Stimulation of this signaling axis in endothelial cells was shown to promote endothelial migration [35]. While PI3K is not predicted to bind to PLXNA1 and PLXNA2, a Scansite [36] analysis of the intracellular domains predicts a possible function for one of the two sites we have identified here. Scansite suggests that PLXNA2 Y1605 phosphorylation could provide a binding site for the SH2 domain of the

adaptor molecule Crk, or its relative CrkL, which preferentially bind to phosphorylated YXXP motifs [37]. The Rap1-GEF C3G binds to the SH3 domain of Crk and CrkL, and is involved in many cellular processes including cell-cell interactions, integrin-mediated adhesion, and differentiation [38]. Thus, Crk and CrkL binding to phosphorylated PlxnA2 could mediate some of the individual roles of Sema signaling. In spite of the fact that SFKs themselves harbor the name-sake SH2 domain, they do not appear to use their SH2 domains to bind to PlxnA receptors as Fyn has been reported to be constitutively bound to PlxnA2 independent of Fyn's kinase activity, and by extension, the tyrosine phosphorylation state of PlxnA2 [22]. Future work will work to identify the proteins that bind to PLXNA proteins at the Fyn-induced phosphorylation sites.

Although the mechanisms downstream of these phosphorylation sites are unknown, the identification of Fyn-dependent PlxnA phosphorylation sites has been anticipated for some time [21]. Here, we have identified the two predominant sites and have found them to be functionally relevant to PlxnA signaling, setting the stage for future steps in delineating the role of tyrosine phosphorylation in PlxnA signaling pathways.

4. Materials and Methods

4.1. Bioinformatics and Multiple Sequence Alignments

Previously reported human PLXNA2 and PLXNA1 tyrosine phosphorylation from large-scale proteomic screens was collected from PhosphoSitePlus [25] (Cell Signaling Technology, Danvers, MA, USA). The conservation of PlxnA2 Y1605 and Y1677 was determined by aligning PlxnA2 and PlxnA1 for vertebrates and invertebrates: human (PLXNA2: NP_079455.3; PLXNA1: NP_115618.3), mouse (PlxnA2: NP_032908.2; PlxnA1: NP_032907.1), rat (PlxnA2: NP_001099458.2; PlxnA1: XP_002729444.2), chicken (PlxnA2: XP_015154528.1; PlxnA1: XP_414370.4), zebrafish (PlxnA2: BAD35133.1; PlxnA1a: XP_003201265.4; PlxnA1b: NP_001103480.1), fruit fly (PlxnA: NP_524637.2), and roundworm (PlxnA: BAB85224.1). Alignments were done using MUSCLE [39] in Geneious version 10.1 (Biomatters, Auckland, New Zealand).

4.2. Plasmids, Cell Culture, and Transfections

The human *PLXNA2* construct (Origene Technologies, Rockville, MD, USA) harbored human *PLXNA2* (NP_079455) containing a C-terminal Myc and Flag tag in pCMV6-Entry. The cloning sites were SgfI and MluI. BioBasic (Markham, Ontario, Canada) produced the single and double point mutant *PLXNA2* constructs: *Y1605F, Y1677F*, and *Y1605F/Y1677F*. BioBasic also synthesized human *PLXNA1-WT* and *PLXNA1-Y1608F/Y1679F* (*Y2F*) containing a C-terminal Myc and Flag tag and cloned them into the vector pUC57. BioBasic cloned *PLXNA1-WT* into pCMV6-Entry vector using SgfI and MluI. To develop a pCMV6-*PLXNA1-Y2F* construct, we used MluI and BssHII (New England Biolabs, Ipswich, MA, USA) to subclone a portion of *PLXNA1* containing *Y1608F/Y1679F* from pUC57-*PLXNA1-Y2F* into pCMV6-Entry-*PLXNA1-WT*. Human *Fyn-WT* (plasmid #16032) and kinase dead mutant *L299M Fyn* (plasmid #16033) constructs were purchased from Addgene (Cambridge, MA, USA), which were originally cloned into pRK5 and deposited by Dr. Filippo Giancotti [40]. HEK293 cells were maintained in DMEM with L-

glutamine, 4.5 g/L glucose and sodium pyruvate (MediaTech/Corning Life Sciences, Tewksbury, MA, USA) supplemented with 5% Fetal Bovine Serum (Hyclone, Logan, UT, USA), 5% Cosmic Calf Serum (Hyclone), 50 units/mL penicillin and 50 μg/mL streptomycin (Invitrogen, Carlsbad, CA, USA) at 37 °C and 5.0% CO_2. Calcium phosphate-based transfections were conducted on cells grown to 75% of confluence. Following a 6-hour incubation, the cells were washed with warm PBS and incubated for an additional 18–20 hours in full medium prior to lysis.

4.3. Cell Lysis, Immunoprecipitation, and Western Blotting

After transfection, cells were placed on ice, washed with cold PBS, and lysed in lysis buffer (25 mM Tris pH 7.4, 137 mM NaCl, 10% glycerol, 1% Igepal) containing protease inhibitors (5 μg/mL Pepstatin, 10 μg/mL Leupeptin, 1 mM PMSF) and phosphatase inhibitors (1 mM $NaVO_3$, 25 mM NaF, 10 mM $Na_2H_2P_2O_7$). Cell extracts were prepared for SDS-PAGE, immunoblotting and immunoprecipitation as previously described [41]. A Bradford Assay [42] was performed to determine protein concentration and extracts were normalized with lysis buffer. Depending on the experiment, between 20 and 30 μg of total protein extract was used for immunoblotting. Depending on the experiment, between 750 and 1,000 μg total protein was used for immunoprecipitations and was incubated overnight at 4 °C with 10 μl of a 50% slurry of α-Flag M2 affinity resin (Sigma-Aldrich Corp., St. Louis, MO, USA) pre-washed with lysis buffer. Immune complexes were washed three times with lysis buffer, drained, and then denatured in protein sample buffer at 95 °C for 5 minutes prior to SDS-PAGE separation. The following primary antibodies and dilutions were used: α-Fyn (rabbit mAb, 1:2000, Cell Signaling Technology), α-Flag M2 (mouse mAb, 1:2000, Sigma-Aldrich Corp.), α-phosphotyrosine 4G10 (mouse mAb; 1:1000, EMD Millipore, Billerica, MA, USA), and α-Src pY416 (rabbit mAb, 1:5000, Cell Signaling Technology). The following secondary antibodies were used: α-rabbit-HRP (goat IgG, 1:15,000, EMD Millipore), α-mouse-HRP (goat IgG, 1:5,000, EMD Millipore), or for immunoprecipitation samples α-mouse-HRP Light Chain Specific (goat IgG, 1:10,000, Jackson ImmunoResearch Laboratories, West Grove, PA, USA). Immunoblotting was performed as described previously [41].

4.4. Enhanced Chemiluminescence, Densitometry Analysis, and Statistics

Proteins from Western Blotting were detected using enhanced chemiluminescence (ThermoFisher Scientific, Waltham, MA, USA) and film was developed using a Medical Film Processor SRX-101A (Konica Minolta Medical & Graphic, Tokyo, Japan). The raw film scans were converted to grayscale and inverted in Adobe Photoshop for densitometry analysis using the mean histogram tool. The background ("untransfected control" group) signal was subtracted from all bands and the tyrosine phosphorylated PLXNA2 or A1 (as measured by α-phosphotyrosine 4G10) levels were made relative to PLXNA2 or A1 + Fyn WT in each experiment by setting this value as 100%. Total PLXNA2 or A1 protein levels were made relative in a similar fashion using α-Flag M2 lanes. Relative α-phosphotyrosine 4G10 levels were then divided by the relative α-Flag M2 levels to calculate the PLXNA2 or A1 tyrosine phosphorylation per sample type. To account for relative Fyn activity, α-phosphotyrosine (4G10) or α-Src pY416 levels for Fyn (as a proxy for kinase activity) were made relative with the levels in the co-transfected Fyn with PLXNA1 or PLXNA2 WT set as

100% in each experiment. The relative PLXNA2 or A1 tyrosine phosphorylation levels were then divided by the relative levels of phosphotyrosyl-Fyn to calculate the final relative tyrosine phosphorylation levels of PLXNA2 or A1. These values were then Log2 transformed and a Student's T-Test pair-wise comparison was performed on the data from three independent experiments using JMP Pro 12 Statistical Software (SAS Institute, Cary, NC, USA).

4.5. Sample Preparation for Mass Spectrometry and Mass Spectrometry Data Analysis

HEK293 cells either untransfected or expressing PLXNA2-WT-Flag and either Fyn WT or Fyn KD were lysed and extracts were subjected to immunoprecipitation with α-Flag M2 affinity resin as described above. Samples were loaded onto 10% SDS-PAGE gels and proteins were visualized using coomassie stain (0.1% coomassie brilliant blue R-250, 20% glacial acetic acid, 40% methanol). The gel region containing the visible PLXNA2-Flag band and corresponding to approximately 200 kDa was cut out, diced, and prepared for tryptic digestion as previously described [43] with the reduction and alkylation steps being omitted. Proteins were subjected to in-gel digestion with 6 ng/μL sequencing-grade modified trypsin (Promega, Madison, WI, USA) in 50 mM ammonium bicarbonate at 37 °C for 6–9 hours. The tryptic peptides were resuspended in Solvent A (2.5% acetonitrile, 0.15% formic acid) and separated via HPLC prior to MS/MS analysis on a linear ion trap-orbitrap (LTQ-Orbitrap) mass spectrometer controlled with Thermo Xcalibur 2.1 software. Peptides were loaded onto 15 cm × 100 μm columns packed with 5 μm C18 packing material (Bruker Daltonics, Billerica, MA, USA, pore size = 200 Å) over 15 minutes in Solvent A and eluted using a 0–50% gradient of Solvent B (99.85% acetonitrile, 0.15% formic acid) over 38 minutes and electrosprayed (2.1 kV) into the mass spectrometer. This gradient was followed by 3 minutes of a 50–100% gradient of Solvent B. This was followed by 4 minutes at 100% Solvent B before a 10-minute equilibration in 100% Solvent A. The precursor scan (scan range = 360–1700 *m/z*, resolution = 3.0×10^4, scan speed = 0.3 Hz) was followed by four collision-induced dissociation (CID) tandem mass spectra. CID spectra were acquired for the top two ions in the precursor scan (isolation window = ±2.0 *m/z*, collision energy = 35 eV), followed by two targeted scans. The targeted scans targeted the average mass (+/− 1.6 *m/z*) of the doubly-charged tryptic peptide ions harboring: (i) the unphosphorylated PLXNA2 Y1605 peptide (791.859 *m/z*, QTSSYNIPASASISR); and (ii) the phosphorylated (pY, underlined) PLXNA2 Y1605 peptide (831.842 *m/z*, QTSSpYNIPASASISR). Dynamic exclusion of precursor ions for MS/MS was enabled with a repeat count of 2, repeat duration of 30 seconds, and exclusion duration of 120 seconds. Theoretical *m/z* values were determined using the Fragment Ion Calculator from the Proteomics Toolkit (Institute for Systems Biology, Seattle, WA, USA). Synthetic tryptic peptides (Cell Signaling Technology) harboring unphosphorylated and phosphorylated Y1605 were added prior to the LC-MS/MS runs. The synthetic peptides were distinguishable from the native given they contained a $^{13}C_5$-, ^{15}N-proline residue increasing the mass by 6.0138 Da. Both manual examination using Thermo Xcalibur's Qual Browser as well as SEQUEST searches were used to interrogate tandem mass spectra. SEQUEST searches queried the forward and reversed concatenated human 2011 Uniprot proteome. The search parameters required tryptic peptides, permitted a precursor *m/z* tolerance of +/− 20 ppm and allowed amino acid modifications of serine, threonine, and tyrosine (+79.9663 Da for phosphorylation), cysteine

(+71.0371 Da for acrylamidation), and methionine (+15.9949 Da for oxidation). SEQUEST peptide identifications were required to be within a false discovery cutoff of 1%.

For the Stable-Isotope Labeling of Amino Acids in Cell Culture (SILAC) experiment, HEK293 cells were grown in $^{13}C_6$-,$^{15}N_4$-labeled arginine and $^{13}C_6$-,$^{15}N_2$-labeld lysine ("heavy condition") as previously described [44]. These cells were transfected as described above with expression plasmids encoding PLXNA2 WT-Flag and Fyn KD. HEK293 cells grown in DMEM containing no heavy-labeled amino acids ("light condition") were transfected with expression plasmids encoding PLXNA2 WT-Flag and Fyn WT. Following lysis, PLXNA2-Flag was immunoprecipitated from each cell state using α-Flag resin. Immune complexes from the two states were combined and subjected to SDS-PAGE. The coomassie-stained PLXNA2 band and the corresponding control derived from untransfected cells were cut and prepared for mass spectrometry analysis as detailed above. Peptides were subjected to LC-MS/MS in a linear ion trap-orbitrap run as previously described [45]. SEQUEST search parameters allowed a precursor ion mass tolerance of 30 ppm, required peptides to be tryptic and allowed for the same amino acid modifications as described above with the addition of arginine (+10.008 for the heavy label) and lysine (+8.014 for the heavy label). Following an automated calculation of the heavy:light ratio [29], the average heavy:light fold change was calculated from unphosphorylated peptides that were fully tryptic and contained no internal arginines or lysines.

4.6. Immunofluorescence in Cell Culture

HEK293 cells were transfected in 6 cm dishes at 75% of confluence with 0.25 μg of either *PLXNA2-WT-Flag* or *PLXNA2-Y2F-Flag* using calcium phosphate precipitation as previously described [46]. COS7 cells were seeded onto glass coverslips in 6-well plates and transfected at 20% of confluence using polyethylenimine [47] and incubated at 37 °C and 5.0% CO_2 for 48 hours. NIE-115 cells were seeded onto poly-L-lysine treated coverslips and transfected at 90% of confluence with Lipofectamine 2000 (ThermoFisher Scientific). Both COS7 and NIE-115 cells were transfected with 2 μg of either *PLXNA2-WT-Flag* or *PLXNA2-Y2F-Flag* and incubated at 37 °C and 5.0% CO_2 for 48 hours. HEK293, NIE-115, and COS7 cells were then processed for immunofluorescence as previously described [46]. The primary antibody was incubated at room temperature for 1 hour in a humidified chamber: α-Flag M2 (mouse mAb, 1:5000, Sigma-Aldrich) in 1.5% BSA in PBS. The secondary antibody was incubated for 45 minutes at 4 °C in a humidified chamber: α-mouse Alexa Fluor 488 (1:10,000, Molecular Probes/Invitrogen). Coverslips were mounted onto microscope slides using VectaShield Hardset mounting media with DAPI (Vector Laboratories, Burlingame, CA, USA). Cells were imaged at 40× magnification using a Nikon Eclipse Ti inverted confocal microscope (Nikon Instruments, Melville, NY, USA). Raw image files were converted to TIFs using ImageJ version 1.48a (National Institutes of Health, USA) and color processing was done in Adobe Photoshop CS6 (San Jose, CA, USA).

4.7. Zebrafish husbandry, Morpholino and mRNA Rescue Experiments

Zebrafish embryos were developmentally staged as previously described [48]. The zebrafish used in this study (*isl2b*:GFP transgenic line) were generously provided by Dr. Chien

(University of Utah, USA). All procedures were approved by the University of Vermont Institutional Animal Care and Use Committee (IACUC). For morpholino injections, 2 ng of a splice-blocking morpholino (MO) (Gene Tools, Philomath, OR, USA) targeting *plxnA2* and/or 200 pg of full-length human *PLXNA2* or *PLXNA2 Y2F* mRNA was injected at the one-cell stage as previously described [7]. The *plxnA2* MO sequence was as follows: AAAAGCGATGTCTTTCTCACCTTCC, which targeted the exon 2-intron 2 boundary. The *plxnA2* MO knock-down efficiency has been previously validated using RT-PCR, and off-target effects and MO specificity have been addressed by rescue of morphant phenotypes with full length human *PLXNA2* mRNA and co-injection of *plxnA2* and *p53* MOs [7, 18]. A second non-overlapping MO construct reproduced the same phenotypes [18]. Capped and tailed full-length mRNA was generated from the pCMV6-Entry-*PLXNA2-WT* and *-Y2F* plasmids by linearizing the plasmids using PmeI (New England Biolabs), T7 RNA polymerase (mMESSAGE mMACHINE kit, Ambion, Austin, TX, USA), and the ThermoFisher PolyA Tailing Kit. These constructs were injected or co-injected with MO into zebrafish embryos at the one-cell stage [48]. Zebrafish embryos were incubated at 28.5 °C for 2 days until the 48 hours post fertilization (hpf) stage [48]. Measurements and brightfield images taken at 6.3× magnification were obtained using SPOT imaging software version 5.2 (Sterling Heights, MI, USA). To account for any variations in overall embryo size, eye size was calculated as eye diameter normalized to head size, which was defined as the distance from the anterior tip of the head to the posterior otic placode [7]. Figures were compiled using Adobe Photoshop CS6, where image brightness was optimized. Graphs and statistical analyses were obtained using Prism 6 (GraphPad Software, La Jolla, CA, USA).

Acknowledgments

We thank D. Jaworski for generously providing NIE-115 cells. This work was supported by U.S. National Science Foundation (NSF) IOS grants 1021795 and 1625154; NSF DBI REU grant 1262786; the Vermont Genetics Network through U. S. National Institutes of Health (NIH) Grant 8P20GM103449 from the INBRE program of the NIGMS; and U.S. NIH Grant 5P20RR016435 from the COBRE program of the NIGMS.

Abbreviations

hpf	hours post fertilization
MO	morpholino
PlxnA	PlexinA
RPC	Retinal Precursor Cell
RTK	receptor tyrosine kinase
Sema6A	Semaphorin6A
SFK	Src Family Kinase
SILAC	Stable Isotope Labeling of Amino Acids in Cell Culture

References

1. Maestrini E, Tamagnone L, Longati P, Cremona O, Gulisano M, Bione S, Tamanini F, Neel BG, Toniolo D, Comoglio PM. A family of transmembrane proteins with homology to the MET-hepatocyte growth factor receptor. Proc Natl Acad Sci U S A. 1996; 93:674–678. [PubMed: 8570614]
2. Jongbloets BC, Pasterkamp RJ. Semaphorin signalling during development. Development. 2014; 141:3292–3297. DOI: 10.1242/dev.105544 [PubMed: 25139851]
3. Kruger RP, Aurandt J, Guan KL. Semaphorins command cells to move. Nat Rev Mol Cell Biol. 2005; 6:789–800. DOI: 10.1038/nrm1740 [PubMed: 16314868]
4. Pasterkamp RJ, Peschon JJ, Spriggs MK, Kolodkin AL. Semaphorin 7A promotes axon outgrowth through integrins and MAPKs. Nature. 2003; 424:398–405. DOI: 10.1038/nature01790 [PubMed: 12879062]
5. Takegahara N, Takamatsu H, Toyofuku T, Tsujimura T, Okuno T, Yukawa K, Mizui M, Yamamoto M, Prasad DV, Suzuki K, et al. Plexin-A1 and its interaction with DAP12 in immune responses and bone homeostasis. Nat Cell Biol. 2006; 8:615–622. DOI: 10.1038/ncb1416 [PubMed: 16715077]
6. Bagnard D, Vaillant C, Khuth ST, Dufay N, Lohrum M, Puschel AW, Belin MF, Bolz J, Thomasset N. Semaphorin 3A-vascular endothelial growth factor-165 balance mediates migration and apoptosis of neural progenitor cells by the recruitment of shared receptor. J Neurosci. 2001; 21:3332–3341. [PubMed: 11331362]
7. Emerson SE, St Clair RM, Waldron AL, Bruno SR, Duong A, Driscoll HE, Ballif BA, McFarlane S, Ebert AM. Identification of target genes downstream of Semaphorin6A/PlexinA2 signaling in zebrafish. Dev Dyn. 2017; doi: 10.1002/dvdy.24512
8. Battistini C, Tamagnone L. Transmembrane semaphorins, forward and reverse signaling: have a look both ways. Cell Mol Life Sci. 2016; 73:1609–1622. DOI: 10.1007/s00018-016-2137-x [PubMed: 26794845]
9. Chauvet S, Cohen S, Yoshida Y, Fekrane L, Livet J, Gayet O, Segu L, Buhot MC, Jessell TM, Henderson CE, et al. Gating of Sema3E/PlexinD1 signaling by neuropilin-1 switches axonal repulsion to attraction during brain development. Neuron. 2007; 56:807–822. DOI: 10.1016/j.neuron.2007.10.019 [PubMed: 18054858]
10. Mauti O, Sadhu R, Gemayel J, Gesemann M, Stoeckli ET. Expression patterns of plexins and neuropilins are consistent with cooperative and separate functions during neural development. BMC Dev Biol. 2006; 6:32.doi: 10.1186/1471-213X-6-32 [PubMed: 16846494]
11. Yang T, Terman JR. Regulating small G protein signaling to coordinate axon adhesion and repulsion. Small GTPases. 2013; 4:34–41. DOI: 10.4161/sgtp.22765 [PubMed: 23247636]
12. Tamagnone L, Artigiani S, Chen H, He Z, Ming GI, Song H, Chedotal A, Winberg ML, Goodman CS, Poo M, et al. Plexins are a large family of receptors for transmembrane, secreted, and GPI-anchored semaphorins in vertebrates. Cell. 1999; 99:71–80. [PubMed: 10520995]
13. Murakami Y, Suto F, Shimizu M, Shinoda T, Kameyama T, Fujisawa H. Differential expression of plexin-A subfamily members in the mouse nervous system. Dev Dyn. 2001; 220:246–258. DOI: 10.1002/1097-0177(20010301)220:3<246::AID-DVDY1112>3.0.CO;2-2 [PubMed: 11241833]
14. Perala NM, Immonen T, Sariola H. The expression of plexins during mouse embryogenesis. Gene Expr Patterns. 2005; 5:355–362. DOI: 10.1016/j.modgep.2004.10.001 [PubMed: 15661641]
15. Takahashi T, Fournier A, Nakamura F, Wang LH, Murakami Y, Kalb RG, Fujisawa H, Strittmatter SM. Plexin-neuropilin-1 complexes form functional semaphorin-3A receptors. Cell. 1999; 99:59–69. [PubMed: 10520994]
16. Toyofuku T, Zhang H, Kumanogoh A, Takegahara N, Suto F, Kamei J, Aoki K, Yabuki M, Hori M, Fujisawa H, et al. Dual roles of Sema6D in cardiac morphogenesis through region-specific association of its receptor, Plexin-A1, with off-track and vascular endothelial growth factor receptor type 2. Genes Dev. 2004; 18:435–447. DOI: 10.1101/gad.1167304 [PubMed: 14977921]
17. Matsuoka RL, Chivatakarn O, Badea TC, Samuels IS, Cahill H, Katayama K, Kumar SR, Suto F, Chedotal A, Peachey NS, et al. Class 5 transmembrane semaphorins control selective Mammalian retinal lamination and function. Neuron. 2011; 71:460–473. DOI: 10.1016/j.neuron.2011.06.009 [PubMed: 21835343]

18. Ebert AM, Childs SJ, Hehr CL, Cechmanek PB, McFarlane S. Sema6a and Plxna2 mediate spatially regulated repulsion within the developing eye to promote eye vesicle cohesion. Development. 2014; 141:2473–2482. DOI: 10.1242/dev.103499 [PubMed: 24917502]
19. Janssen BJ, Robinson RA, Perez-Branguli F, Bell CH, Mitchell KJ, Siebold C, Jones EY. Structural basis of semaphorin-plexin signalling. Nature. 2010; 467:1118–1122. DOI: 10.1038/nature09468 [PubMed: 20877282]
20. Nogi T, Yasui N, Mihara E, Matsunaga Y, Noda M, Yamashita N, Toyofuku T, Uchiyama S, Goshima Y, Kumanogoh A, et al. Structural basis for semaphorin signalling through the plexin receptor. Nature. 2010; 467:1123–1127. DOI: 10.1038/nature09473 [PubMed: 20881961]
21. Franco M, Tamagnone L. Tyrosine phosphorylation in semaphorin signalling: shifting into overdrive. EMBO Rep. 2008; 9:865–871. DOI: 10.1038/embor.2008.139 [PubMed: 18660749]
22. Sasaki Y, Cheng C, Uchida Y, Nakajima O, Ohshima T, Yagi T, Taniguchi M, Nakayama T, Kishida R, Kudo Y, et al. Fyn and Cdk5 mediate semaphorin-3A signaling, which is involved in regulation of dendrite orientation in cerebral cortex. Neuron. 2002; 35:907–920. [PubMed: 12372285]
23. Mitsui N, Inatome R, Takahashi S, Goshima Y, Yamamura H, Yanagi S. Involvement of Fes/Fps tyrosine kinase in semaphorin3A signaling. Embo J. 2002; 21:3274–3285. DOI: 10.1093/emboj/cdf328 [PubMed: 12093729]
24. Catalano A, Lazzarini R, Di Nuzzo S, Orciari S, Procopio A. The plexin-A1 receptor activates vascular endothelial growth factor-receptor 2 and nuclear factor-kappaB to mediate survival and anchorage-independent growth of malignant mesothelioma cells. Cancer Res. 2009; 69:1485–1493. DOI: 10.1158/0008-5472.CAN-08-3659 [PubMed: 19176370]
25. Hornbeck PV, Zhang B, Murray B, Kornhauser JM, Latham V, Skrzypek E. PhosphoSitePlus, 2014: mutations, PTMs and recalibrations. Nucleic Acids Res. 2015; 43:D512–520. DOI: 10.1093/nar/gku1267 [PubMed: 25514926]
26. Swiercz JM, Worzfeld T, Offermanns S. Semaphorin 4D signaling requires the recruitment of phospholipase C gamma into the plexin-B1 receptor complex. Mol Cell Biol. 2009; 29:6321–6334. DOI: 10.1128/MCB.00103-09 [PubMed: 19805522]
27. Morita A, Yamashita N, Sasaki Y, Uchida Y, Nakajima O, Nakamura F, Yagi T, Taniguchi M, Usui H, Katoh-Semba R, et al. Regulation of dendritic branching and spine maturation by semaphorin3A-Fyn signaling. J Neurosci. 2006; 26:2971–2980. DOI: 10.1523/JNEUROSCI.5453-05.2006 [PubMed: 16540575]
28. Ong SE, Blagoev B, Kratchmarova I, Kristensen DB, Steen H, Pandey A, Mann M. Stable isotope labeling by amino acids in cell culture, SILAC, as a simple and accurate approach to expression proteomics. Mol Cell Proteomics. 2002; 1:376–386. [PubMed: 12118079]
29. Matsuoka S, Ballif BA, Smogorzewska A, McDonald ER 3rd, Hurov KE, Luo J, Bakalarski CE, Zhao Z, Solimini N, Lerenthal Y, et al. ATM and ATR substrate analysis reveals extensive protein networks responsive to DNA damage. Science. 2007; 316:1160–1166. DOI: 10.1126/science.1140321 [PubMed: 17525332]
30. Suto F, Tsuboi M, Kamiya H, Mizuno H, Kiyama Y, Komai S, Shimizu M, Sanbo M, Yagi T, Hiromi Y, et al. Interactions between plexin-A2, plexin-A4, and semaphorin 6A control lamina-restricted projection of hippocampal mossy fibers. Neuron. 2007; 53:535–547. DOI: 10.1016/j.neuron.2007.01.028 [PubMed: 17296555]
31. Zhuang B, Su YS, Sockanathan S. FARP1 promotes the dendritic growth of spinal motor neuron subtypes through transmembrane Semaphorin6A and PlexinA4 signaling. Neuron. 2009; 61:359–372. DOI: 10.1016/j.neuron.2008.12.022 [PubMed: 19217374]
32. Polleux F, Morrow T, Ghosh A. Semaphorin 3A is a chemoattractant for cortical apical dendrites. Nature. 2000; 404:567–573. DOI: 10.1038/35007001 [PubMed: 10766232]
33. van Horck FP, Lavazais E, Eickholt BJ, Moolenaar WH, Divecha N. Essential role of type I(alpha) phosphatidylinositol 4-phosphate 5-kinase in neurite remodeling. Curr Biol. 2002; 12:241–245. [PubMed: 11839279]
34. Wang H, Hota PK, Tong Y, Li B, Shen L, Nedyalkova L, Borthakur S, Kim S, Tempel W, Buck M, et al. Structural basis of Rnd1 binding to plexin Rho GTPase binding domains (RBDs). J Biol Chem. 2011; 286:26093–26106. DOI: 10.1074/jbc.M110.197053 [PubMed: 21610070]

35. Basile JR, Afkhami T, Gutkind JS. Semaphorin 4D/plexin-B1 induces endothelial cell migration through the activation of PYK2, Src, and the phosphatidylinositol 3-kinase-Akt pathway. Mol Cell Biol. 2005; 25:6889–6898. DOI: 10.1128/MCB.25.16.6889-6898.2005 [PubMed: 16055703]
36. Obenauer JC, Cantley LC, Yaffe MB. Scansite 2.0: Proteome-wide prediction of cell signaling interactions using short sequence motifs. Nucleic Acids Res. 2003; 31:3635–3641. [PubMed: 12824383]
37. Ballif BA, Carey GR, Sunyaev SR, Gygi SP. Large-scale identification and evolution indexing of tyrosine phosphorylation sites from murine brain. J Proteome Res. 2008; 7:311–318. DOI: 10.1021/pr0701254 [PubMed: 18034455]
38. Bos JL, de Rooij J, Reedquist KA. Rap1 signalling: adhering to new models. Nat Rev Mol Cell Biol. 2001; 2:369–377. DOI: 10.1038/35073073 [PubMed: 11331911]
39. Edgar RC. MUSCLE: multiple sequence alignment with high accuracy and high throughput. Nucleic Acids Res. 2004; 32:1792–1797. DOI: 10.1093/nar/gkh340 [PubMed: 15034147]
40. Mariotti A, Kedeshian PA, Dans M, Curatola AM, Gagnoux-Palacios L, Giancotti FG. EGF-R signaling through Fyn kinase disrupts the function of integrin alpha6beta4 at hemidesmosomes: role in epithelial cell migration and carcinoma invasion. J Cell Biol. 2001; 155:447–458. DOI: 10.1083/jcb.200105017 [PubMed: 11684709]
41. Weir ME, Mann JE, Corwin T, Fulton ZW, Hao JM, Maniscalco JF, Kenney MC, Roman Roque KM, Chapdelaine EF, Stelzl U, et al. Novel autophosphorylation sites of Src family kinases regulate kinase activity and SH2 domain-binding capacity. FEBS Lett. 2016; 590:1042–1052. DOI: 10.1002/1873-3468.12144 [PubMed: 27001024]
42. Bradford MM. A rapid and sensitive method for the quantitation of microgram quantities of protein utilizing the principle of protein-dye binding. Anal Biochem. 1976; 72:248–254. [PubMed: 942051]
43. Cheerathodi M, Vincent JJ, Ballif BA. Quantitative comparison of CrkL-SH3 binding proteins from embryonic murine brain and liver: Implications for developmental signaling and the quantification of protein species variants in bottom-up proteomics. J Proteomics. 2015; 125:104–111. DOI: 10.1016/j.jprot.2015.04.033 [PubMed: 25982384]
44. Buel GR, Rush J, Ballif BA. Fyn promotes phosphorylation of collapsin response mediator protein 1 at tyrosine 504, a novel, isoform-specific regulatory site. J Cell Biochem. 2010; 111:20–28. DOI: 10.1002/jcb.22659 [PubMed: 20506281]
45. Aten TM, Redmond MM, Weaver SO, Love CC, Joy RM, Lapp AS, Rivera OD, Hinkle KL, Ballif BA. Tyrosine phosphorylation of the orphan receptor ESDN/DCBLD2 serves as a scaffold for the signaling adaptor CrkL. FEBS Lett. 2013; 587:2313–2318. DOI: 10.1016/j.febslet.2013.05.064 [PubMed: 23770091]
46. Arnaud L, Kelley LP, Helias V, Cartron JP, Ballif BA. SMIM1 is a type II transmembrane phosphoprotein and displays the Vel blood group antigen at its carboxyl-terminus. FEBS Lett. 2015; 589:3624–3630. DOI: 10.1016/j.febslet.2015.09.029 [PubMed: 26452714]
47. Boussif O, Lezoualc'h F, Zanta MA, Mergny MD, Scherman D, Demeneix B, Behr JP. A versatile vector for gene and oligonucleotide transfer into cells in culture and in vivo: polyethylenimine. Proc Natl Acad Sci U S A. 1995; 92:7297–7301. [PubMed: 7638184]
48. Kimmel CB, Ballard WW, Kimmel SR, Ullmann B, Schilling TF. Stages of embryonic development of the zebrafish. Dev Dyn. 1995; 203:253–310. DOI: 10.1002/aja.1002030302 [PubMed: 8589427]

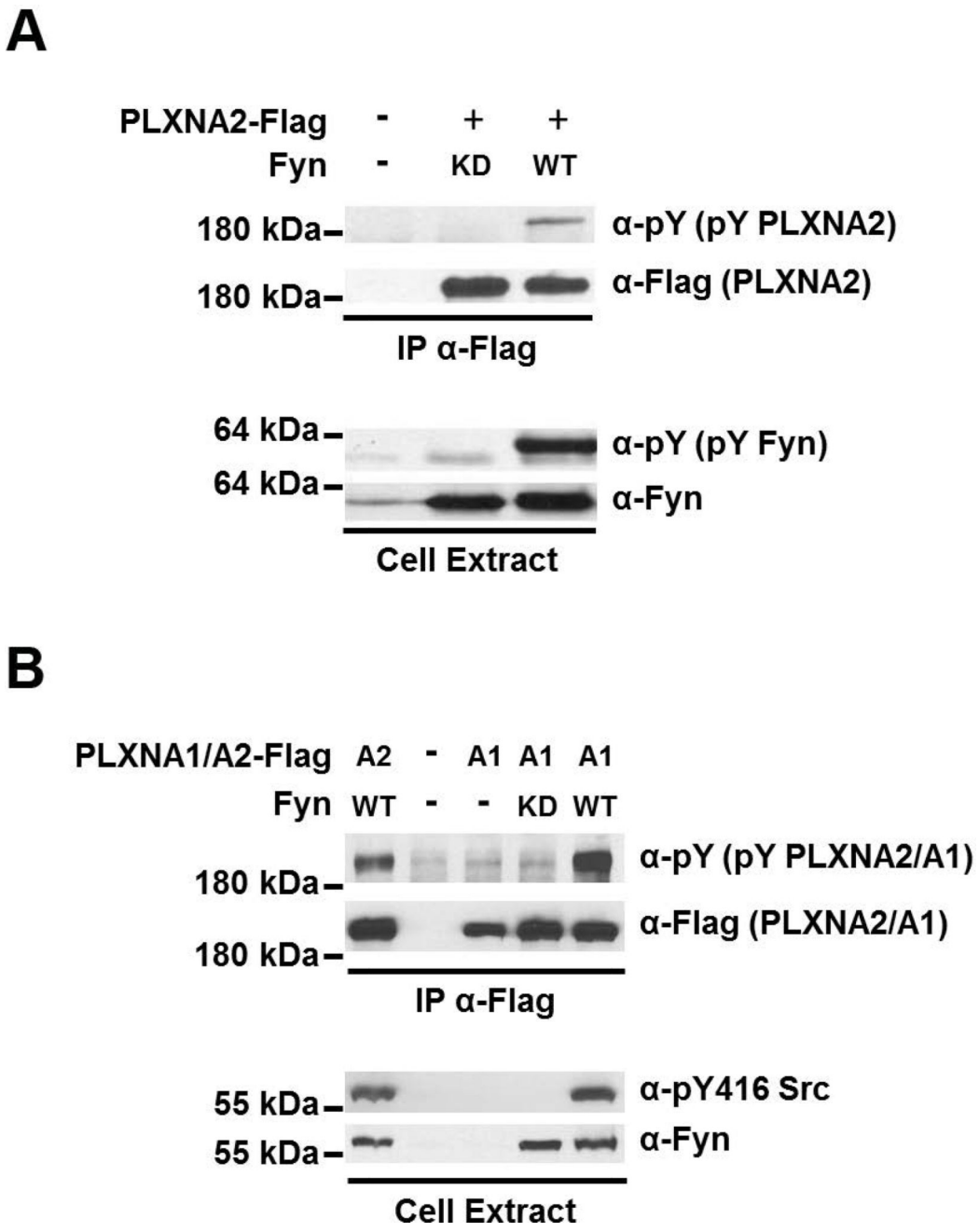

Figure 1. Fyn Induces PLXNA2 and PLXNA1 Phosphorylation

(A–B) HEK293 cells were transfected with expression plasmids encoding PLXNA2-Flag, PLXNA1-Flag, Fyn wildtype (WT) or Fyn kinase dead (KD) as indicated. Cell extracts were subjected to immunoprecipitation with α-Flag resin. Immune complexes and whole cell extracts were subjected to SDS-PAGE and immunoblotting with the indicated antibodies.

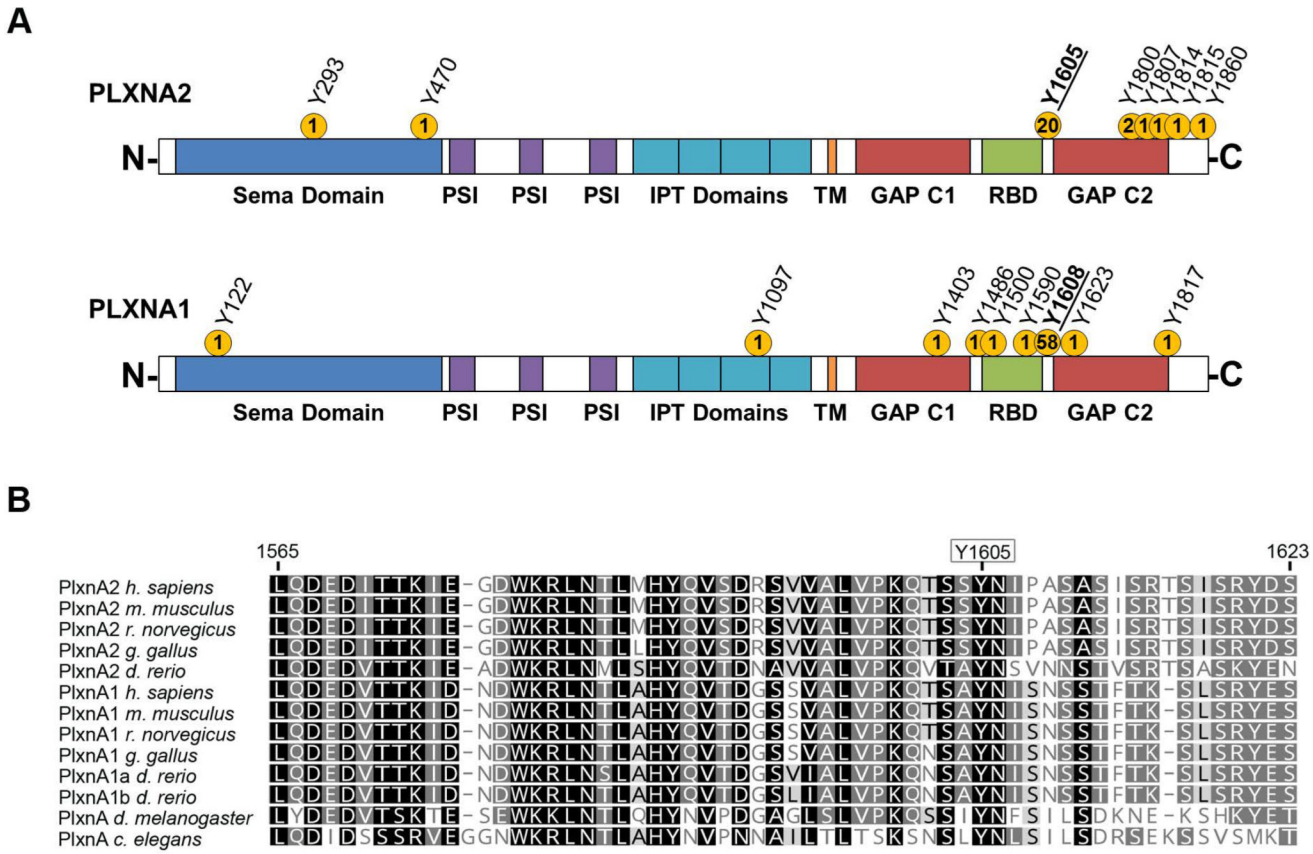

Figure 2. Bioinformatic Analysis Identifies a Conserved Tyrosine Phosphorylation Site in PlxnA2 and PlxnA1

(A) PhosphoSitePlus curation shows 20 large-scale mass spectrometry records of human PLXNA2 Y1605 being phosphorylated (top) and 58 records of phosphorylation at the homologous site Y1608 in human PLXNA1 (bottom). Plxns are single-pass type I transmembrane proteins and the N-terminal extracellular and the C-terminal intracellular domain structures are displayed. PSI: plexin, semaphorin, integrin domain; IPT: Ig-like, plexin, transcription factors domain; TM: transmembrane; GAP C1/2: split Ras-GTPase-activating protein domains; RBD: Rho family GTPase-binding domain (B). A sequence alignment highlights the conservation of PlxnA2 Y1605 across vertebrates and invertebrates as well as among PlxnA1 family members. Accession numbers are as follows: human PLXNA2: NP_079455.3, mouse PlxnA2: NP_032908.2, rat PlxnA2: NP_001099458.2, chicken PlxnA2: XP_015154528.1, zebrafish PlxnA2: BAD35133.1, human PLXNA1: NP_115618.3, mouse PlxnA1: NP_032907.1, rat PlxnA1: XP_002729444.2, chicken PlxnA1: XP_414370.4, zebrafish PlxnA1a: XP_003201265.4, zebrafish PlxnA1b: NP_001103480.1, fruit fly PlxnA: NP_524637.2, and roundworm PlxnA: BAB85224.1.

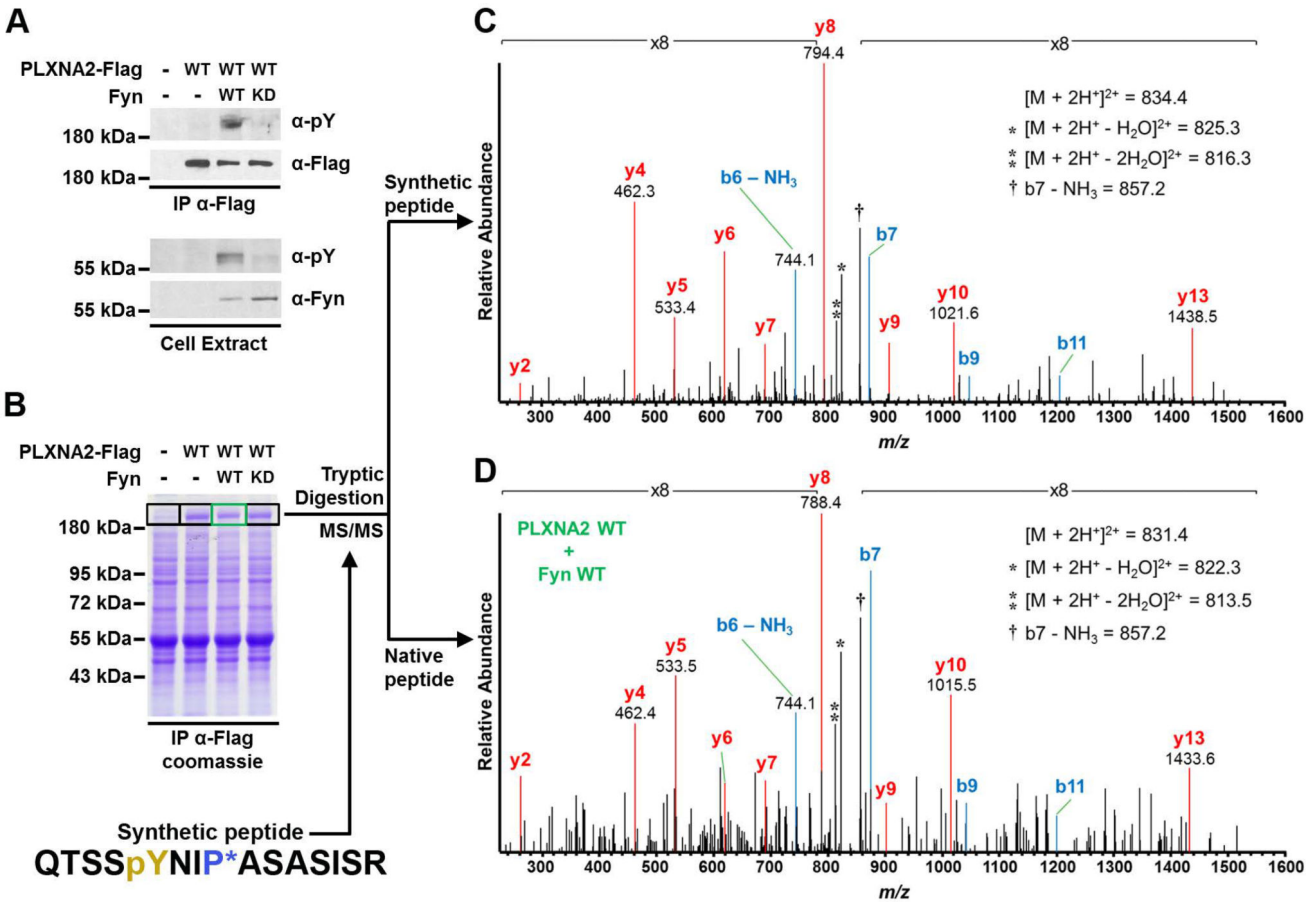

Figure 3. Targeted Mass Spectrometry Reveals Y1605 as a Fyn-Induced Phosphorylation Site on PLXNA2

HEK293 cells were transfected with expression plasmids encoding PLXNA2-Flag, Fyn wildtype (WT) or Fyn kinase dead (KD) as indicated. Whole cell extracts were subjected to immunoprecipitation with α-Flag resin. (A) Whole cell extracts and a small fraction of the immune complexes were subjected to SDS-PAGE and immunoblotting with the indicated antibodies. (B) The majority of the immune complexes for each sample was subjected to SDS-PAGE and protein bands were visualized by coomassie staining. The regions of the gel where PLXNA2 bands run were excised and digested with trypsin and the tryptic peptides were prepared for mass spectrometry. Unphosphorylated and phosphorylated Y1605-containing synthetic reference peptides with a $^{13}C_5$- and ^{15}N-labeled proline (P*) were added to the native extracted peptides. A targeted approach was used to subject the appropriate *m/z* values of the doubly-charged tryptic peptides containing either the unphosphorylated or phosphorylated Y1605 to Collision-Induced Dissociation in a linear ion trap-orbitrap mass spectrometer. (C–D) The unphosphorylated native PLXNA2 peptide containing Y1605 was found across treatment groups, but the phosphorylated native peptide was only found in the PLXNA2 + Fyn WT group. Shown are the MS/MS spectra of the phosphorylated Y1605 synthetic peptide (C) and the Y1605 phosphorylated native peptide (D).

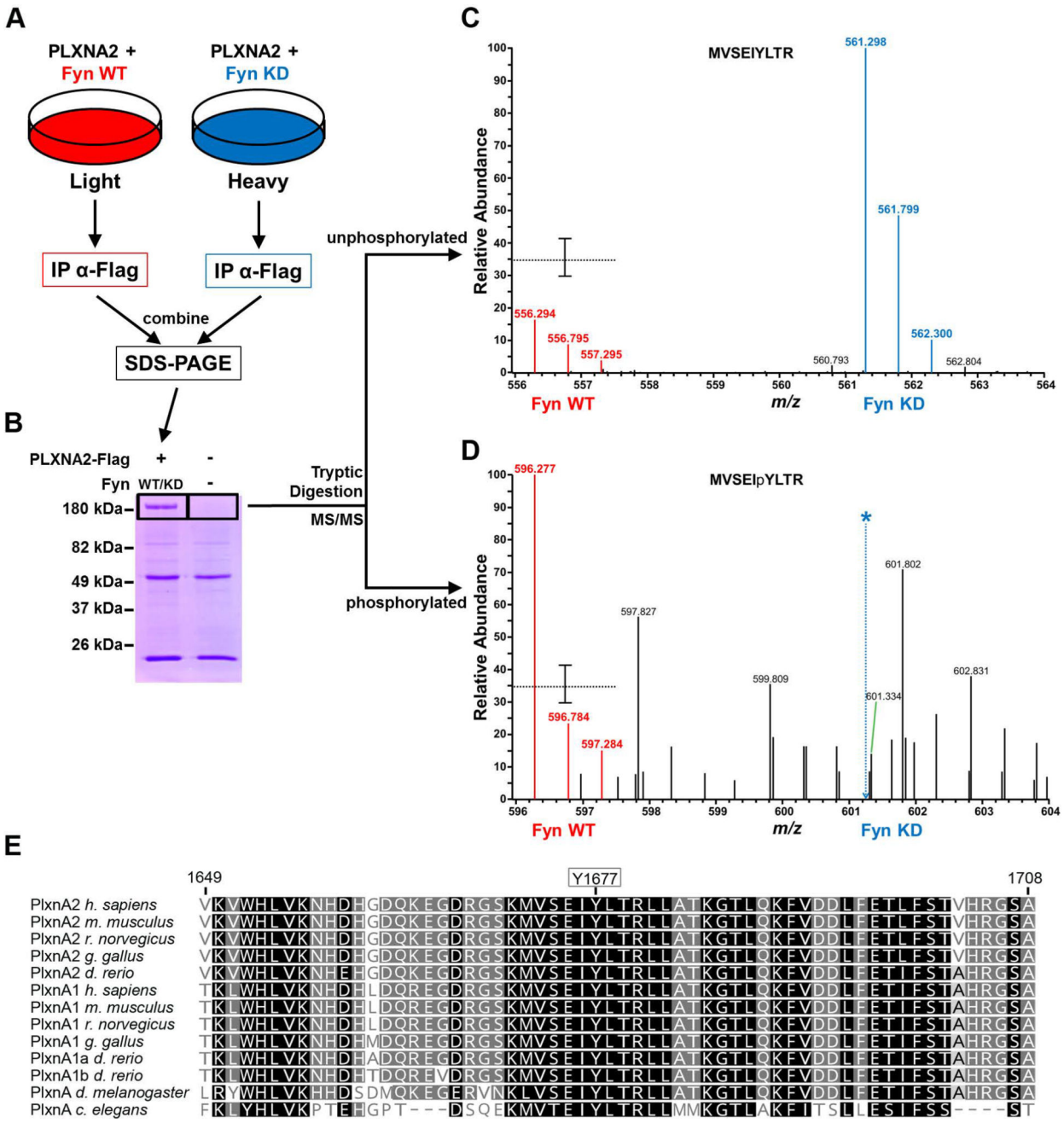

Figure 4. Y1677 is a Novel Fyn-Dependent PLXNA2 Phosphorylation Site

(A) Diagram showing the SILAC design to identify PLXNA2 phosphorylation sites dependent on Fyn kinase activity. (B) Coomassie-stained gel of proteins immunoprecipitated from SILAC cell extracts. The region of the gel corresponding to approximately 200 kDa was cut out from experimental and control lanes, subjected to in-gel tryptic digestion and run on a linear ion trap-orbitrap mass spectrometer. (C–D) MS1 *m/z* windows harboring the isotopic envelopes of the SILAC pairs of tryptic peptide precursor ions of PLXNA2 unphosphorylated at Y1677 (556–564) (C) or phosphorylated at Y1677 596–604 (D). The red peaks represent the isotopic envelopes of the light PLXNA2 peptide precursor ions, or

those from the + Fyn WT condition. The blue peaks represent the isotopic envelopes of the heavy PLXNA2 peptide precursor ions, or those from the + Fyn KD condition. The blue, dashed line (bottom) indicates the expected value of the monoisotopic peak of the phosphorylated PLXNA2 precursor peptide ion, which was not present (m/z = 601.282). The black dashed line in both spectra represents the mean heavy:light fold change (mean = 2.87 +/− 0.48 fold change; n = 71, errors bars indicate s.d.) of all other fully tryptic PLXNA2 peptide ions identified. (D) Multiple sequence alignment showing the position of Y1677 across several model organisms for both PlxnA2 as well as PlxnA1.

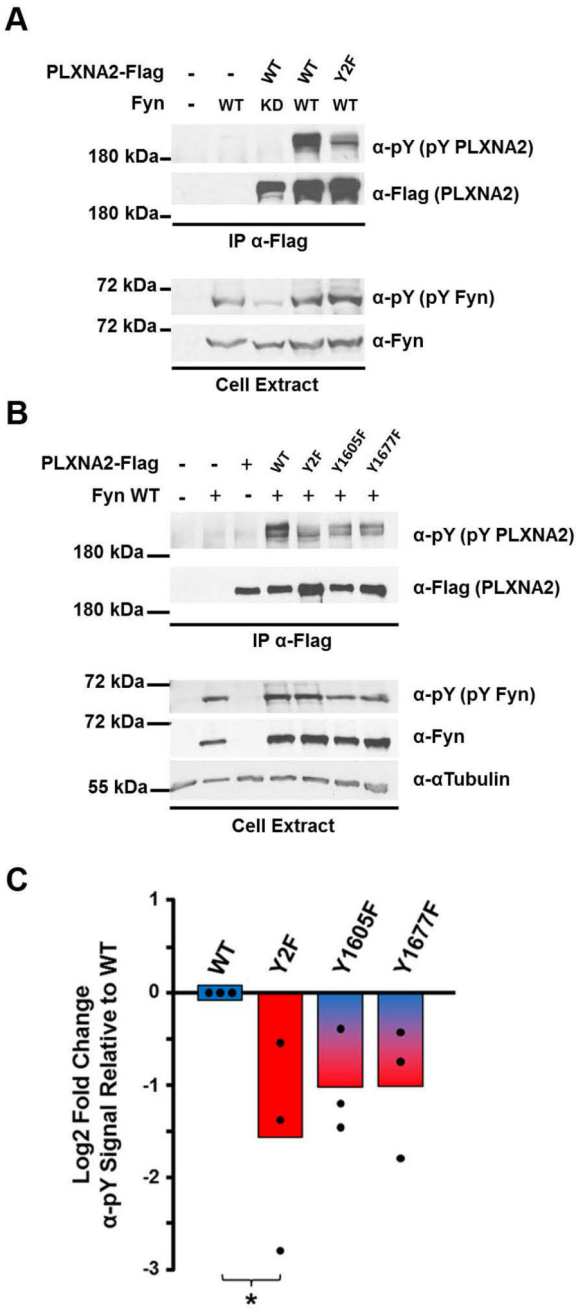

Figure 5. Y1605 and Y1677 are the Major Sites of Fyn-Induced PLXNA2 Tyrosine Phosphorylation

(A–B). HEK293 cells were co-transfected with Fyn WT and Flag-tagged expression constructs for either PLXNA2 WT or the PLXNA2 tyrosine-to-phenylalanine mutants Y2F (Y1605F/Y1677F), Y1605F, or Y1677F. PLXNA2 was immunopurified by α-Flag resin and subjected to SDS-PAGE and immunoblotting with the indicated antibodies. (C) The relative decrease in overall tyrosine phosphorylation normalized to PLXNA2 WT + Fyn WT was quantified for each sample type. Histograms show the average of three independent experiments. *Students T-Test, p = 0.029.

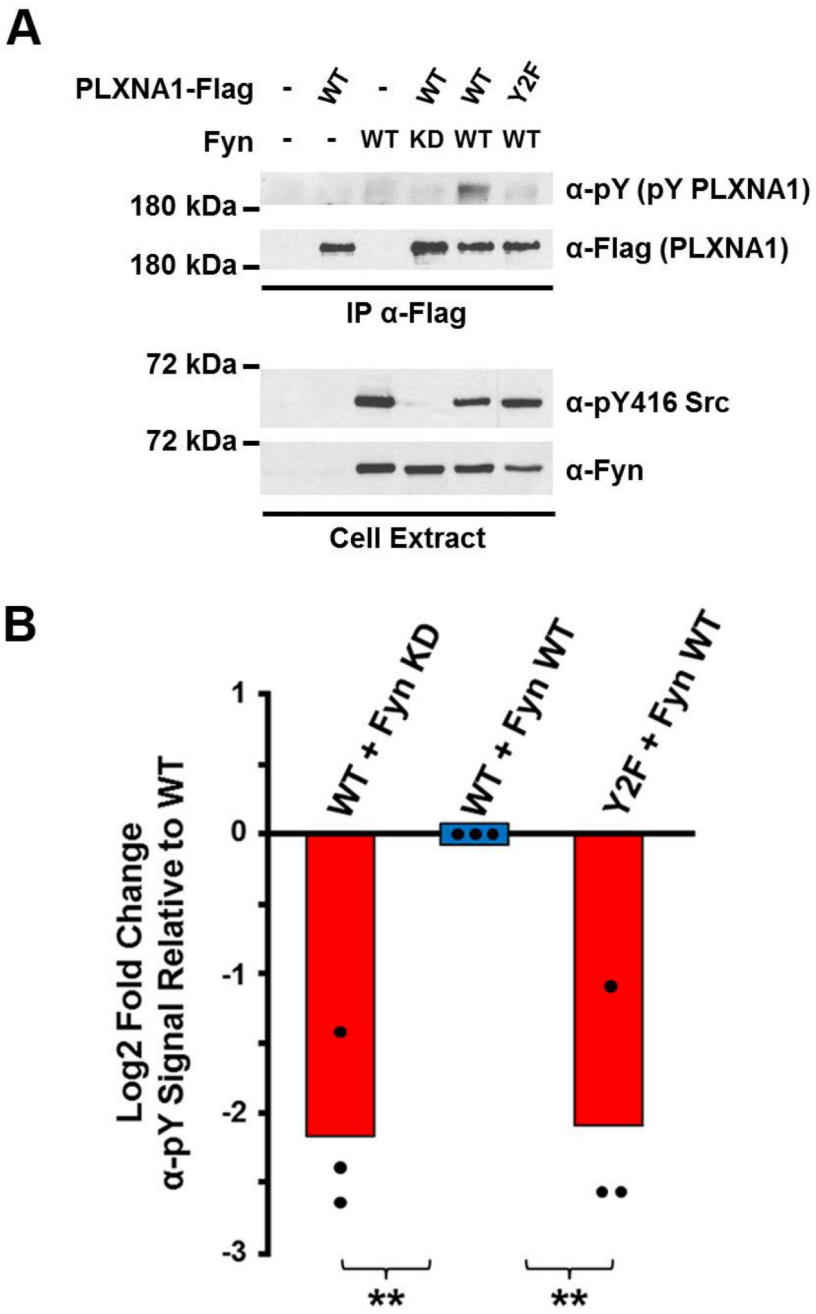

Figure 6. Y1608 and Y1679 are the Major Fyn-Induced Sites of PLXNA1 Tyrosine Phosphorylation

(A). HEK293 cells were co-transfected with Fyn WT or Fyn KD and Flag-tagged expression constructs for either PLXNA1 WT or the PLXNA1 tyrosine-to-phenylalanine Y2F mutant (Y1608F/Y1679F). PLXNA1 was immunopurified by α-Flag resin and subjected to SDS-PAGE and immunoblotting with the indicated antibodies. (B) The relative decrease in overall tyrosine phosphorylation normalized to PLXNA1 WT + Fyn WT was quantified for each sample type. Histograms show the average of three independent experiments. **Students T-Test, WT + Fyn WT comparison to WT + Fyn KD $p = 0.005$; WT + Fyn WT comparison to Y2F + Fyn WT $p = 0.006$.

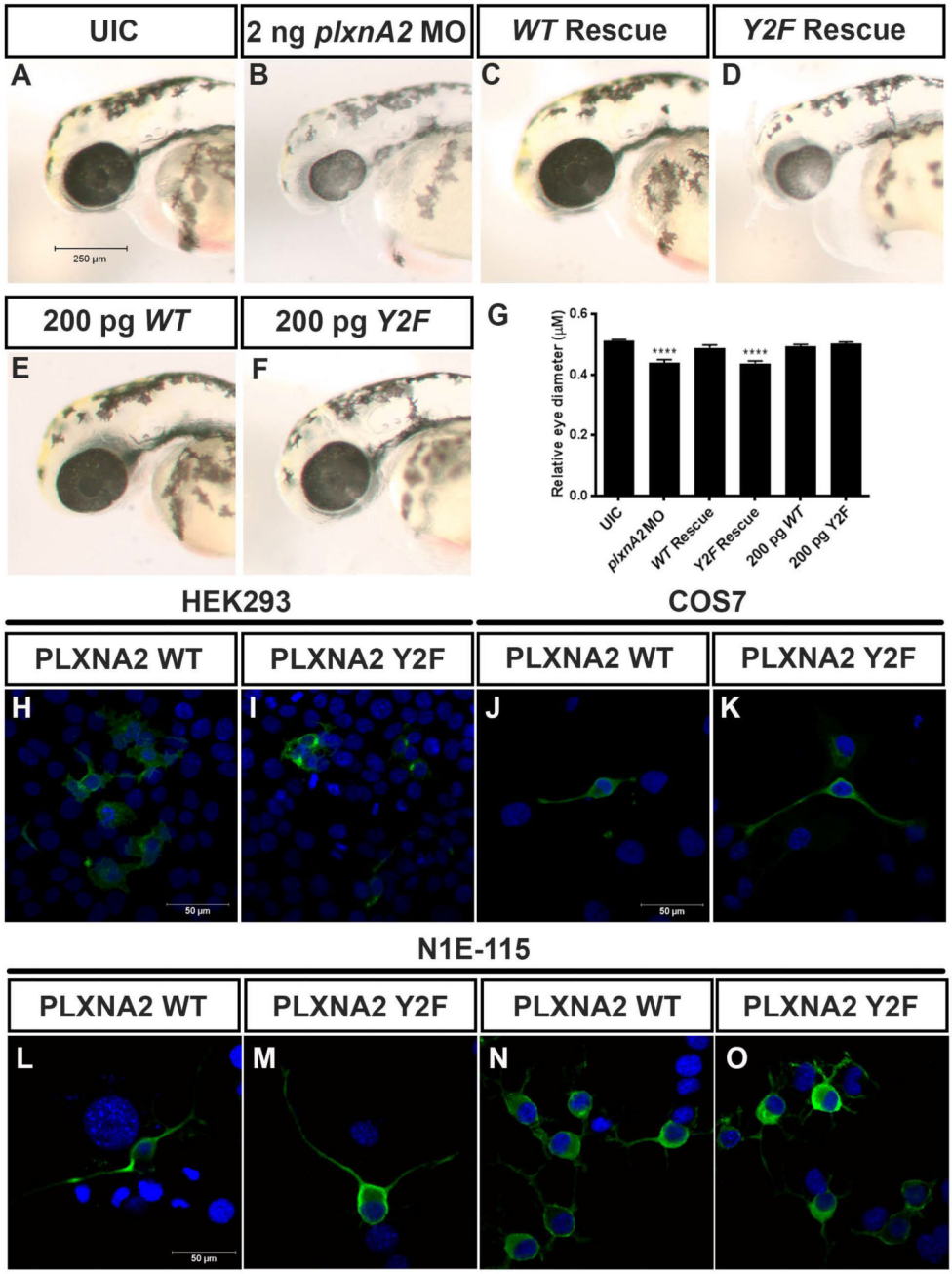

Figure 7. Fyn-dependent PlxnA2 tyrosine phosphorylation sites are essential for zebrafish eye development

(A–F) Brightfield images of zebrafish embryos at 48 hours post fertilization (hpf). (A, B, G) *PlxnA2* morphants showed a reduction in eye size compared to uninjected control (eye diameter relative to head length (Control 0.513 µm +/−0.003 µm, n=40 N=4; *PlxnA2* MO 0.439 µm +/−0.009 µm, n=40 N=4, ****P<0.0001)). (C, D, G) Co-injection of 2 ng *plxna2* MO with 200 pg full-length human *PLXNA2-WT* mRNA rescued the small eye phenotype, however, full-length human *PLXNA2-Y2F* mRNA was unable to rescue eye size when co-injected with 2 ng *plxna2* MO (Control 0.513 µm +/−0.003 µm, n=40 N=4; *WT* rescue 0.488 µm +/−0.008 µm, n=34 N=4, n.s; *Y2F* rescue 0.437 µm +/−0.007 µm, n= 40 N=4,

****P<0.0001). (E, F, G) No observed difference in eye size was seen with overexpression of 200 pg *WT* or *Y2F* full-length human mRNA (Control 0.513 μm +/−0.003 μm, n=40 N=4; 200 pg *WT* 0.493 μm +/−0.005 μm, n=30 N=3, n.s; 200 pg *Y2F* 0.502 μm +/−0.005 μm, n=30 N=3, n.s). One-way ANOVA, multiple comparisons test. Error bars indicate s.e.m. UIC: uninjected control, MO: morpholino, hpf: hours post fertilization. (H–O) PLXNA2 WT and Y2F show similar subcellular localization in HEK293, COS7, and NIE-115 cells, cell lines that have been used in Sema-Plxn signaling studies. NIE-115 cells show similar PLXNA2 WT and Y2F localization patterns in cells with both long and short processes (L–O). Green is PLXNA2 and blue is DAPI.